

THE POPULATION STRUCTURE OF THE LARGE MAGELLANIC CLOUD BAR

EDUARDO HARDY¹

Département de physique and Observatoire du Mont Mégantic, Université Laval

ROBERTO BUONANNO AND CARLO E. CORSI

Osservatorio Astronomico di Roma

KENNETH A. JANES²

Astronomy Department, Boston University

AND

ROBERT A. SCHOMMER¹

Department of Physics and Astronomy, Rutgers University

Received 1983 April 29; accepted 1983 August 29

ABSTRACT

We have used a combination of profile-deconvolution and automatized techniques of photographic photometry in crowded fields to construct a rich and deep color-magnitude diagram near the NW end of the Large Magellanic Cloud (LMC) bar. The morphology of the diagram and its analysis through the use of luminosity functions and evolutionary models for the core-helium-burning "clump" red giants indicate that (1) stellar formation continues in the bar areas; (2) an old Population II in the Galaxy sense is not a significant contributor to the observed diagram, although stars of all ages are probably present in the LMC disk; (3) the bulk of star formation, which continues to date, started earlier than about one billion years ago but later than about three billion years ago, although the precise rate of star formation, including the possible presence of bursts, inside such an age range is not known from our data. The observed population is considerably younger and more metal deficient than that of the solar neighborhood.

Subject headings: galaxies: Magellanic Clouds — galaxies: structure — stars: formation — stars: stellar statistics

I. INTRODUCTION

Due to their proximity, the Magellanic Clouds offer the unique possibility of allowing the study of intrinsically faint individual stars in a galactic context other than that of our own Galaxy. The history of star formation can thus be reconstructed, at least in principle, from the analysis of color-magnitude diagrams (CMD) via appropriate evolutionary models. This direct approach contrasts with that adopted, of necessity, in the analysis of more distant, unresolved systems, for which one must rely on integrated photometric and spectroscopic properties. It also points toward studies of resolved systems as calibration stepping-stones for the interpretation of unresolved ones. In this context, it is somewhat surprising to remark the existence of only a few detailed studies of the stellar content of the Magellanic Clouds field as opposed to the rich body of data concerning their cluster systems. This is partly a result of the difficulties inherent in the interpretation of the CMD of noncoeval systems and partly a consequence of the assumption that one needs to penetrate to very faint magnitudes ($M_V \approx +4$) to obtain valid information, a very difficult proposition in very crowded regions.

Studies of faint field stars in the Clouds have recently known a bonanza as a result of the development of new techniques of analysis of faint images in crowded fields incorporating deconvolution algorithms to take care of the

contamination of the stellar profiles due to the superposition of images. Results by Butcher (1977) and more recently by Stryker, Butcher, and Jewell (1981) and Stryker (1983) have shown that in the peripheral regions of the Large Magellanic Cloud (LMC) at distances ranging from 5 to 9 kpc from the center, the bulk of star formation started $3-6 \times 10^9$ yr ago. This might indicate that the "halo" regions of the LMC are of intermediate age and have formed later than at least one of its clusters: NGC 2257 (Stryker 1983). Related studies have now been undertaken in the Small Magellanic Cloud (see Hardy, Melnick, and Rheault 1980; Hardy and Durand 1984).

The central region of the LMC, in particular the bar itself, is of considerable interest for it exhibits a strong concentration of the pervasive sheet of red giants present in all the galaxies of the Local Group (Sandage 1970), and it is the only bar structure that can be resolved from Earth. More importantly, as discussed by Kormendy (1981), bars are responsible for secular evolution effects through interaction with other components in their galaxy. Thus, to the extent to which axial symmetry is the exception rather than the rule, secular evolution may have an important effect in the structure of most galaxies. From a population point of view, the study of a resolved bar is then of considerable interest.

We know of only two photometric investigations into the nature of the LMC bar. Tift and Snell (1971, hereafter TS) constructed CMDs to $V \approx 18$ in an area situated near the NW end of the bar. They predicted that a horizontal branch of Population II would be found if the CMDs were extended past $V = 19.5$, in line with previous contentions that the

¹ Guest Investigator, Mount Wilson and Las Campanas Observatories of the Carnegie Institution of Washington.

² Visiting Astronomer, Cerro Tololo Inter-American Observatory.

observed red giants belonged to a Population II component in the Galaxy sense. Later, Hardy (1977, 1978*a, b*) studied a number of regions in and around the bar proper and concluded, on the basis of CMDs, integrated colors, and luminosity functions, that the presence of an intermediate-age population could not be ruled out.

In the present investigation, we use new large-scale plate material combined with recent techniques of analysis of contaminated stellar profiles in an attempt to construct CMDs in the LMC bar which are deeper and richer than hitherto available.

II. THE DATA

a) Observations and Data Analysis

The same general region studied by TS was selected for our study because (1) it has a "moderate" degree of stellar crowding as it is located near the NW end of the bar, (2) it has a well-determined (albeit bright) stellar sequence, (3) inspection of van den Berghs (1974) UV prints does not reveal the presence of dust lanes, and (4) although near the young clusters NGC 1850, 1854, 1856, and 1858, our region is sufficiently removed from them that contamination is unimportant. The area studied is shown in Figure 1; its integrated photometric characteristics, listed in Table 1, are those of region 5 in Hardy (1978*b*), which it includes. Table 1 also lists, for comparison, some photometric properties of the bar and the LMC general field. In what follows we adopt Sandage and Tammann's (1971) distance scale and reddening: $(m - M)_{AV} = 18.83$; $A_V = 0.24$.

A series of *B* plates (103a-O + W2C) were obtained with the du Pont Telescope at Las Campanas, and another series of *V* plates (IIa-D + GG495) were secured at the CTIO 4 m prime focus. Two deep pairs taken in excellent seeing ($\sim 1''$ FWHM) were selected and digitized in steps of $25 \mu\text{m}$ with the European Southern Observatory PDS at Garching for reduction at the Rome Astronomical Observatory. The density images were then transformed to intensity units using calibration steps (or wedges) and stellar profiles (Moffat 1969; Buonanno *et al.* 1983*a*). The first reduction of the data followed the procedure outlined by Buonanno *et al.* (1979) and Buonanno, Corsi, and Fusi Pecci (1981). An image matrix usually containing a mean of six possible stellar centers was displayed by the computer on a Tektronix graphics terminal, thus allowing the operator to identify visually all the images in the matrix and the most likely position of such centers. The stellar images were then treated with a standard point-spread function (PSF) expressed in intensity units and given by the expression (Moffat 1969)

$$I(r) = I_0 [1 + (r/R)^2]^{-\beta}. \quad (1)$$

Such a profile approximates a Gaussian near the center while reproducing well an exponential behavior near the wings of the images. The parameters R and β were previously determined from well-isolated stars, and the PSF with the central intensity I_0 as a free parameter together with a slanted "sky plane" was then fitted simultaneously to every group displayed. This simultaneous fit to the entire image matrix performs in practice a profile deconvolution and restitutes their true profiles to the contaminated individual objects. The goodness of fit was interactively controlled by displaying "cuts" of the observed and fitted profiles projected in three orthogonal planes. The procedure is interactive in that the identifications of images can be revised if the projected shapes of the profiles indicated that, for example, a faint image in the wing of a brighter one had not been recognized.

This method, developed at the Rome Astronomical Observatory (Buonanno *et al.* 1979), has been widely tested and applied to stellar photometry in heavily populated regions, i.e., globular clusters, always with good results (Buonanno, Corsi, and Fusi Pecci 1981; Buonanno *et al.* 1983*b, c*). Other authors (Butcher 1977; Tody 1980; Stryker 1983) have used analogous techniques in dealing with similar problems in densely packed stellar fields. Transformation of the instrumental magnitudes into the standard Johnson system was obtained via 35 TS standards. The relationship was found to be strictly linear with unit slope and a standard deviation of the residuals of 0.07 mag in both colors over the entire range of almost 5 mag to $V = 18$. No statistically significant color terms were detected. The above stresses the good quality of our density-intensity conversions, also demonstrated by the stability of the parameters R and β of the PSF used in the determination of the magnitudes. This lends confidence to the extrapolation of the calibration line to the plate limit. Furthermore, the linearity and internal accuracy of the reduction procedure were confirmed by the plate-to-plate comparison of the entire data set (1500 stars), which again yielded a linear relationship with $\sigma_V = 0.07$ mag and $\sigma_B = 0.08$ mag over a range of nearly 8 mag.

b) The Color-Magnitude Diagrams

The final CMD for nearly 1500 stars derived through the above procedure is shown in Figure 2, where no reddening corrections have yet been applied to the data. This diagram represents our best efforts in terms of photometric accuracy. Two problems, however, are worth discussing prior to any attempted interpretation of the data. First, sampling problems are readily apparent in the CMD: Is the secondary clumping of stars at $V \approx 18$, $B - V \approx 1.0$ above the main clump at $V \approx 19$, $B - V \approx 0.8$ real? What is the extension toward fainter magnitudes of the main clump: is there a subgiant

TABLE 1
POSITIONS AND INTEGRATED COLORS OF SELECTED FIELDS IN THE LMC

Region	R.A.	Decl.	$B - V$	$U - B$	V_{lim}	Reference
This paper	$\sim 05^{\text{h}}09^{\text{m}}5$	$-68^{\circ}57'$	0.60 ± 0.03	0.05 ± 0.03	21	Hardy 1978 <i>b</i>
Fig. 1 (mean)	0.67 ± 0.06	0.03 ± 0.06	...	Hardy 1978 <i>b</i>
Near NGC 1866	$\sim 05 13.0$	$-65 30$	23	Butcher 1977
Near NGC 1783	$\sim 04 59.0$	$-66 00$	23	Stryker and Butcher 1981
Near NGC 2257	$\sim 06 30.0$	$-64 10$	23	Stryker, Butcher, and Jewell 1981

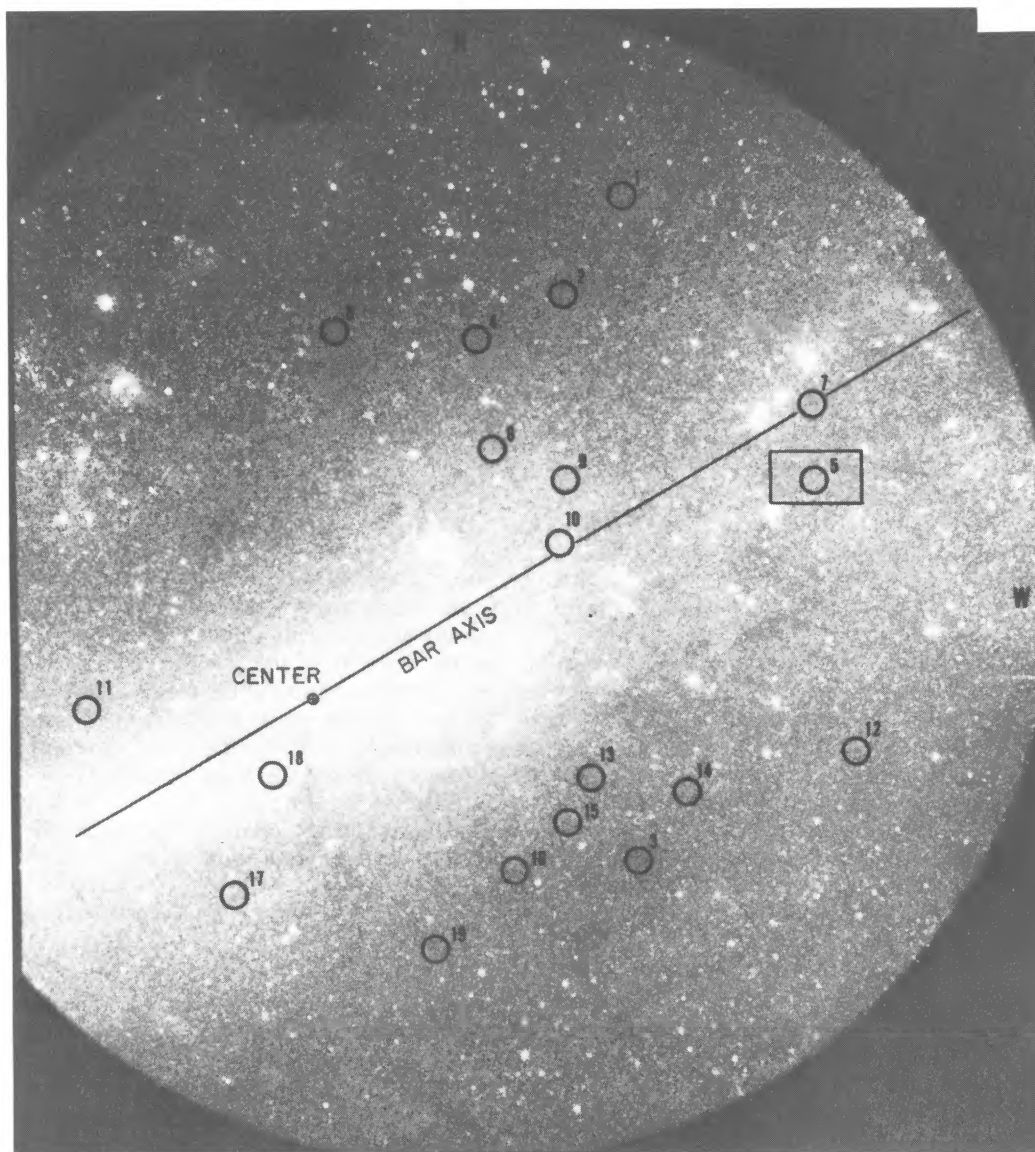


FIG. 1.—The main body of the LMC with the axis of the bar and the centroid of the system of planetary nebulae indicated. The circular regions (3' in diameter) have measured colors and, in some cases, bright CMDs (see Hardy 1978*b* and references therein). The area studied in this investigation is shown as a rectangle of dimensions 6' \times 12' enclosing region 5. The information contained in the areas shown here is partially summarized in Table 1.

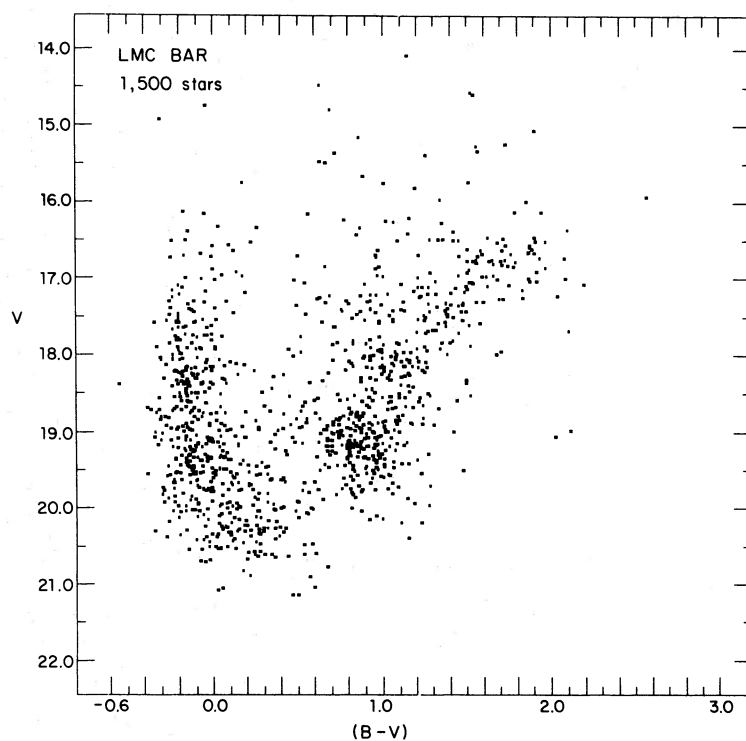


FIG. 2.—The CMD for $\sim 1,500$ stars measured through the profile-deconvolution technique described in the text. No reddening corrections have been applied.

branch? Second, the degree of completeness of the measured sample, essential to the establishment of luminosity functions, is somewhat undetermined, being a function of the degree of contamination of a stellar image, which, in turn, is a function of its magnitude. Fainter than $V \sim 19.5$ it became difficult and laborious to manually identify and control all stellar images because of the impractical amount of human and machine time required by an interactive approach.

In order to increase the size of the sample and to alleviate the completeness problem, we decided to perform a different second reduction of the data. Automatized photometry to the limit of a peak-seeking algorithm was then carried out using the sample of Figure 2 as a photometric control. The procedure adopted was to use the total intensity contained in the central 3×3 pixels of each stellar profile; use of such a small area (roughly the central arcsec) minimizes the effects of crowding in the photometry at the expense of accuracy and, possibly, dynamic range. It provides, however, an efficient and fast way of dealing with a very large sample of stars, which would have been otherwise impractical. Since, on the other hand, it was no longer possible to determine the background through a fit to a "sky plane," the entire area was divided in square subregions of dimension 40×40 pixels, and a common smoothed value of the sky background valid for all stars in that particular subregion was determined from the histogram of pixel intensities (i.e., Bijaoui 1980).

The next step was to use as standards the stars in common with Figure 2. The effect of saturation in the central pixels of bright stars was readily observable as a curvature in the

calibration curve. A polynomial fit to the curve was then obtained and used to recompute the 3×3 pixel magnitudes in the system of the fitted magnitudes of Figure 2. Finally, the residuals were plotted as a function of magnitude over a 7 mag range to $V = 21$ and $B = 22$ in Figure 3. The distribution of residuals indicates that we have reproduced the magnitude scales to within $\sigma = 0.10$ mag. The precision of the 3×3 pixel method is somewhat surprising if one considers the relatively unsophisticated procedure followed in determining the magnitudes as compared with the previous method. One should, however, bear in mind that if the intensity profiles are well represented by equation (1), and if the parameters R and β are constant for a given plate, once the background has been properly determined, the only remaining free parameter is then the value I_0 of the central peak, which is well determined through the use of the central pixels. The losses in statistical precision due to the fewer pixels used are compensated to a large extent by the lesser degree of contamination occurring at the center of the images. The resulting CMD for a total of nearly 18,000 stars is shown in Figures 4 and 5. Figure 5 has been labeled using the parameters of § IIa, i.e., $(m - M)_{AV} = 18.80$ and $E(B - V) = 0.08$, and contains a number of reference observational and theoretical sequences, described in the legend. From visual inspection of randomly selected image matrices at the graphics terminal we estimate our photometry to be complete to better than 10% at the magnitude levels indicated in Figure 5. We did not, however, insert artificial control stellar images in our matrices as was done in Stryker (1983).

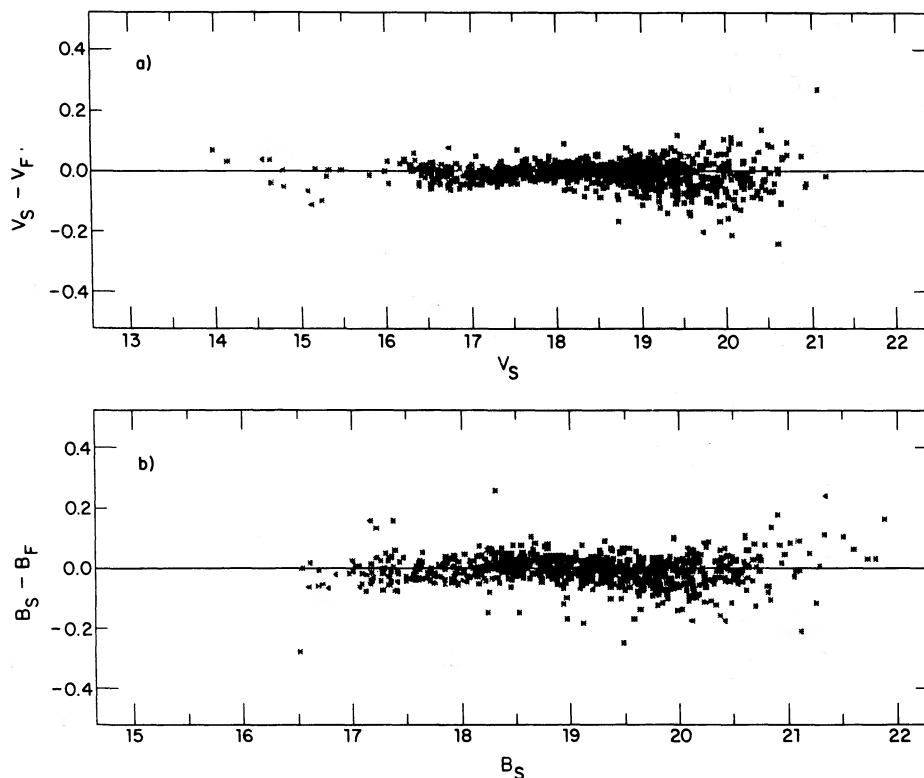


FIG. 3.—Residuals vs. magnitudes from the transformations between the “fitted” magnitudes (F) of Fig. 2 and the “summed” magnitudes (S) of Figs. 4 and 5. (a) Visual data; (b) blue data.

III. ANALYSIS OF THE CMD

a) Global Features

Three features are noteworthy in Figures 4 and 5: (1) a main sequence (MS) extending to bright magnitudes ($V < 16$), (2) a densely populated giant-branch “clump” at $(\langle V \rangle, \langle B - V \rangle) = (19.2, 0.8)$ with full-widths in the magnitude and color axes of approximately 0.6 and 0.4 mag, respectively, and (3) a well-defined giant branch centered at its base with respect to the clump and reaching $V = 16$ and $(B - V) = 2.2$ at its topmost extension. This bright and red extension can be identified with an asymptotic giant branch (AGB) in the Aaronson and Mould (1982) sense.

The presence of a bright MS reflects the fact that stellar formation is an ongoing process in the bar field, although some contamination from the nearby young clusters may be expected. The interpretation of the giants in terms of age of star formation is less clear. They may in principle belong to a combination of the following population types known to exist in the LMC: (1) a bona fide Population II component as typified by NGC 2257 (Stryker 1983), (2) an old halo population (Stryker, Butcher, and Jewell 1981; Butcher 1977), and (3) an intermediate-age disk population (Hardy 1978a; Hodge 1982; Stryker and Butcher 1981). None of these population types are likely to be present exclusively of the others in view of the spread in ages consistent with the observed MS, the presence of RR Lyrae variables (Graham 1973), and the possibility of a LMC halo seen in projection against the presumably flatter bar structure. *It is the question of the relative contributions of these populations which is the*

main subject of this investigation. As an aid in the analysis of Figures 4 and 5 we have generated the corresponding Hess diagram of Figure 6, where the numbers of stars inside bins of size $[\Delta V = 0.1; \Delta(B - V) = 0.05]$ are represented numerically. From there, luminosity functions for specific sequences can be readily obtained, and they are displayed in Table 2 and Figures 7 and 8.

We can safely exclude a significant contribution from an NGC 2257 population (Stryker 1983) because of the obvious color shift shown in Figure 5 between such a sequence and the observed giant branch. We can also exclude an NGC 2257-like population of higher metallicity because of the absence of a subgiant branch of stellar density comparable to that of the clump itself (which would then be interpreted

TABLE 2
MAIN-SEQUENCE AND RED-GIANT LUMINOSITY FUNCTIONS

V	M_V	$\log \phi$ (MS)	$\log \phi$ (RG)
17.05–17.35	–1.60	1.34	1.94
17.35–17.65	–1.30	1.49	2.14
17.65–17.95	–1.00	1.67	2.17
17.95–18.25	–0.70	1.91	2.26
18.25–18.55	–0.40	2.23	2.48
18.55–18.85	–0.10	2.32	2.54
18.85–19.15	0.20	2.52	2.87
19.15–19.45	0.50	2.69	3.01
19.45–19.75	0.80	2.82	2.86
19.75–20.05	1.10	3.03	2.66
20.05–20.35	1.40	3.15	...
20.35–20.65	1.70	3.25	...

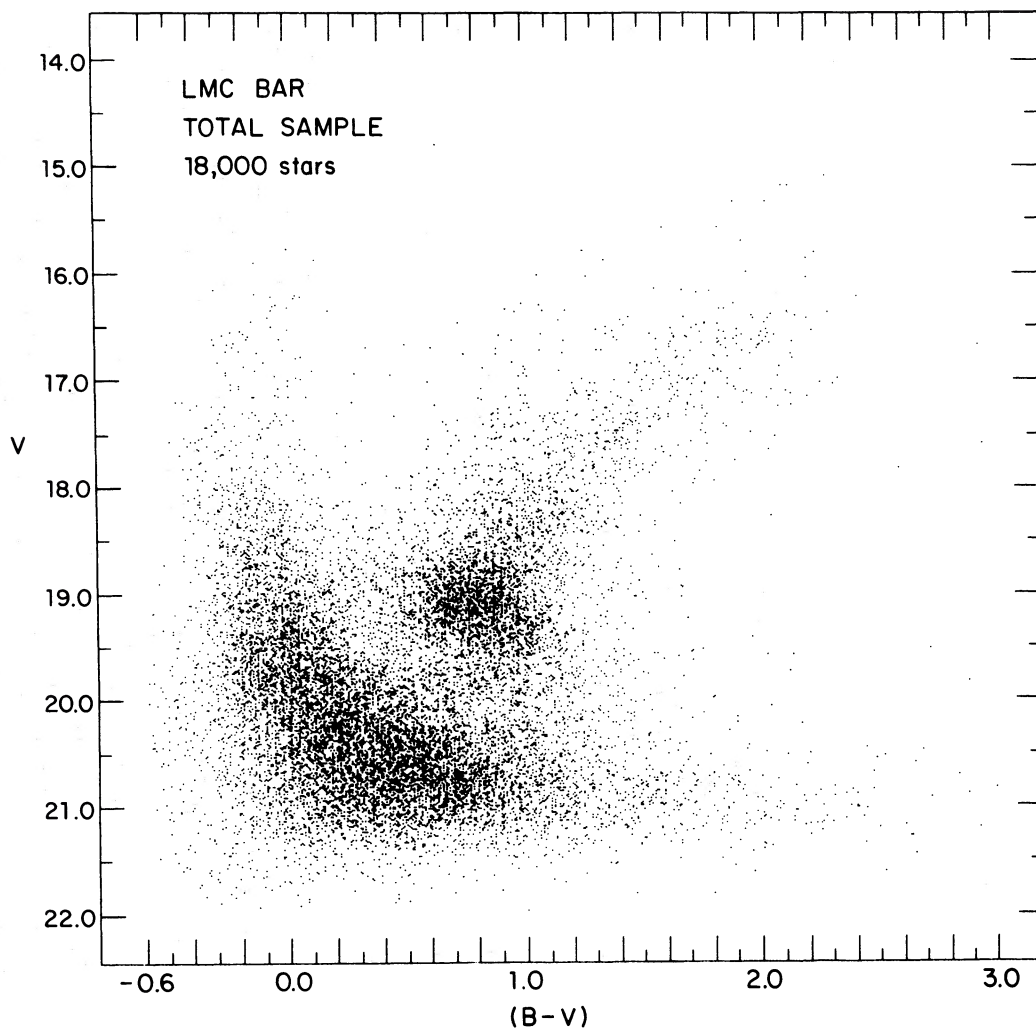


FIG. 4.—The CMD for the entire sample of nearly 18,000 stars measured automatically and calibrated via the sample of Fig. 2. The diagram was generated by an impact printer. Because of this, only one point per resolution element was printed, leading to some incompleteness as a function of the actual population density. The real density contrast of stars between regions in the diagram is somewhat larger than shown (see Fig. 6). No reddening corrections have been applied.

as being a horizontal branch [HB] of Population II). We will show later that most of the points located in the subgiant portion of the CMD arise because of errors in the photometry of faint MS stars as shown by the symmetry of the residuals about the central locus of the MS along lines of faint constant B and V magnitudes. In addition, the presence of a blue HB of the appropriate density would have appeared as a strong “bump” in the MS luminosity function of Figure 7 at $V \approx 19.0$. The argument concerning the subgiant branch coupled to the observed symmetry of the red-giant branch with respect to the center of the clump argues also against the presence of a Population II component à la 47 Tucanae with a “stubby” red HB (see Sandage 1982a for the schematics of the globular cluster CMD). Note also in Figure 5 the location of the NGC 2158 giant branch, which may be representative of the intermediate-age population of the anticenter of the Galaxy (Hardy 1981). Finally, the presence of a well-populated AGB argues in favor of the presence of a strong intermediate-age popula-

tion, whereas the low density of stars near the NGC 188 locus confirms the absence of a significant solar-neighborhood type of population (Hardy 1978a). We now turn to the analysis of the MS and the giant branch in an effort to put more stringent limits on the main ages of star formation.

b) The Main Sequence

The MS luminosity function from this paper is compared in Figure 7 with Sandage’s (1957) initial LF, Mermilliod’s (1981a) Pleiades bright end, and Stryker and Butcher’s (1981) LMC-field LF. From the slope, it is clear that the observed LF is not coeval, and that a superposition of star formation periods is implied. Notice the good agreement in slope with Stryker and Butcher (1981). No clear evidence for a turnoff is present along the MS, except for a small discontinuity at $V = 18.4$; note, however (Fig. 5), that some indications of evolutionary deviations are present at faint magnitudes. But the superposition of ages could be expected to bury the effect of a turnoff by reducing the detection contrast. In

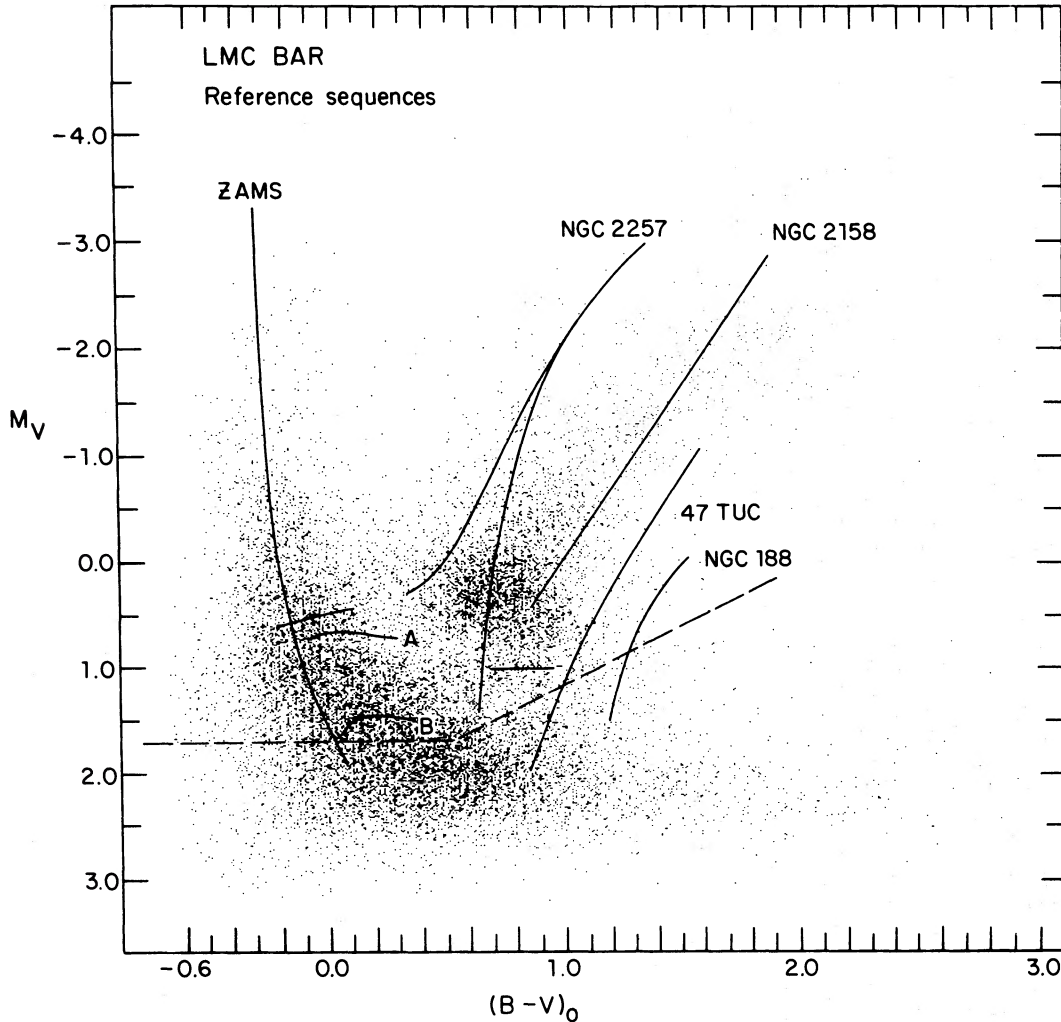


FIG. 5.—Same as Fig. 4 but with reddening and distance modulus applied. Reference sequences are superposed. The dashed lines indicate the V and B confidence limits of the photometry and the stellar counts. Sources are as follows: ZAMS (Mermilliod 1981*b*); NGC 2257 (Stryker 1983); NGC 2158 (Arp and Cuffey 1962); 47 Tuc and NGC 188 (Sandage 1982*b*). Isochrones A ($t = 10^9$ yr, $Z = 0.004$) and B ($t = 2 \times 10^9$ yr, $Z = 0.001$) are from Ciardullo and Demarque (1977).

principle, knowledge of the shape of the initial mass function in the LMC coupled to appropriate evolutionary models may permit modeling of the observed LF. We will not adopt such an approach here but rather will argue that the information contained in the giant branch and particularly in the clump can be used to set limits on the ages of preponderant star formation.

c) The Giant Clump

Figure 8 shows the visual red-giant LF derived from a cut of Figure 4 along the axis of the giant branch. The Gaussian shape of the function near the faint end, centered around $V = 19.2$ ($M_V = 0.4$), is controlled by the clump population. The observed V -magnitude full-width (taken as equal to 2σ of the distribution) is 0.6 mag, which is adopted as the characteristic size of the clump. The corresponding clump population is $N_c = 2100$, from integration under the histogram of Figure 8, with an estimated error of $\pm 10\%$ arising from

Poisson sampling errors and uncertainties in the boundaries of the clump.

Cannon (1970) realized on an empirical basis that the mean absolute magnitude M_V^c of core-helium-burning stars in the giant clump of galactic clusters was correlated with the age of the clusters for objects younger than $\sim 10^9$ yr and near-solar metallicities. Mermilliod (1981*b*) has systematized on a uniform basis all of the presently available photometry for young and intermediate-age clusters in the Galaxy and found a relation of the form

$$\log t = 0.280 M_V^c + 8.61 \quad (2)$$

valid for $\log t \leq 8.8$ (and therefore $M_V^c \sim 0.7$). Past this point the variation of M_V^c must be very slow since for the globular clusters $M_V^c = 0.8$ (Sandage 1982*a*). More recently, Flower (1984) has put this relationship on a firm theoretical basis by studying a grid of stellar evolutionary tracks which he evolved from the MS through core-helium exhaustion

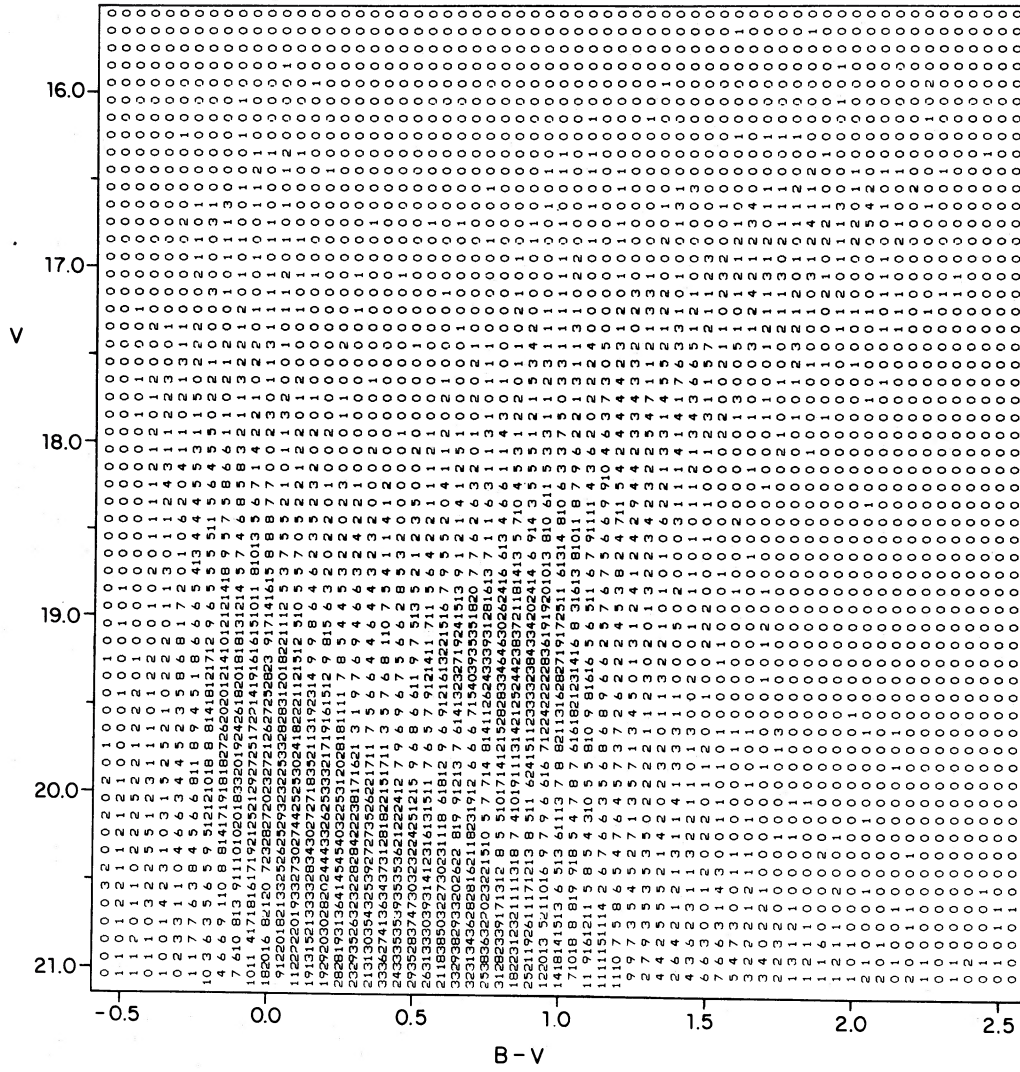


FIG. 6.—A numerical CMD (“Hess diagram”). No reddening corrections have been applied. Data bins are of dimension 0.1 mag in V and 0.05 mag in $B - V$.

spanning a large interval of masses and compositions. He showed that, as expected, there was a luminosity minimum where changes in luminosities and temperatures began to occur on a slow (nuclear) time scale which corresponds to the observed clump on the CMD. Since for a given cluster, the fainter clump members are the least massive ones, their position must map more accurately the present cluster age. Figure 9 presents Mermilliod’s data together with Flower’s models in the $(\log t, M_V)$ -plane. Flower’s models are evaluated at the faint edge (FE) of the clump distribution, whereas Mermilliod’s data are for the mean clump position. Notice that Flower’s models run parallel to the empirical relationship for metallicities between near-solar and $[\text{Fe}/\text{H}] = -0.7$. For this interval in composition his computations for the faintest clump red giants of magnitude M_V^{FE} can be represented by

$$\log t = 0.28 M_V^{\text{FE}} + 8.47. \quad (3)$$

This corresponds to a shift $\Delta \log t = +0.14$ from the FE magnitudes to the M_V^c ones, or, correspondingly, $\Delta M = 0.5$

for t constant. For $[\text{Fe}/\text{H}] = -1$, the slope of the relation is somewhat shallower at

$$\log t = 0.23 M_V^{\text{FE}} + 8.69. \quad (4)$$

The behavior of the models for older stars is not known explicitly, but, on empirical grounds, they must level off very fast past the last point in Figure 9 and converge toward the globular cluster limit, which is labeled (4) in the figure.

In what follows we adopt $[\text{Fe}/\text{H}] = -0.7$ for the metallicity of the LMC disk (Cowley and Hartwick 1982; Hodge 1982). From Figure 9 we find that for such a metallicity the mean clump position at $M_V^c = +0.4$ (or, conversely, the faint edge of the clump at $M_V^{\text{FE}} \approx 0.8$) is near the end of the relationship at $\sim 0.8 \times 10^9$ yr. As discussed, past this point a “funneling” effect maps core-helium-burning red giants of increasing age onto an invariable red clump. Either most stars in the observed LMC clump were formed almost coevally from a narrow portion of the MS—which from the Yale isochrones (Ciardullo and Demarque 1977) must be near $M_V = 0.8$ —or,

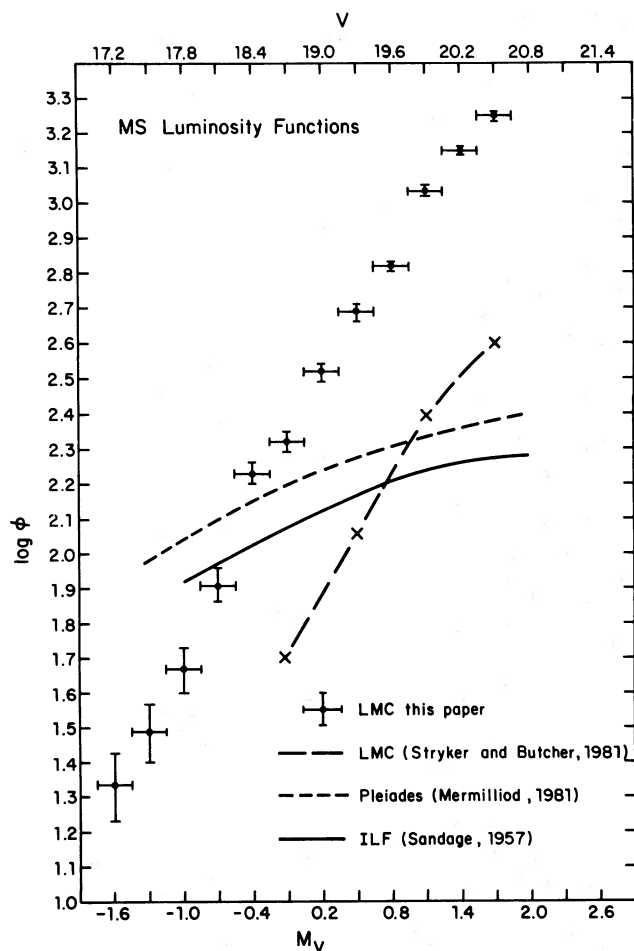


FIG. 7.—The main-sequence differential luminosity functions. All sources are indicated.

rather, older stars have been accumulating which came from a wider range in magnitude along a fainter MS.

We now test the supposition that the preponderant age of star formation happened to be placed at the limit age of Figure 9 near 0.8×10^9 yr by assuming constant $[\text{Fe}/\text{H}]$ and asking whether the magnitude width and the total population of the clump are compatible with a narrow epoch of star formation. From the form of equations (2) and (3) we derive

$$\Delta t/t = 0.65\Delta M. \quad (5)$$

We adopt $\Delta M = 0.6$ as derived from the discussion of Figure 8. Equation (5) then gives $\Delta t/t = 0.4$, which implies that the observed clump may be populated by stars ranging in age from $t - \Delta t/2 = 0.65 \times 10^9$ to $t + \Delta t/2 = 0.95 \times 10^9$ yr. Such an age interval corresponds, again from the Yale isochrones, to an interval of 0.3 mag in termination points along the MS immediately above $M_V = 0.8$. Next we ask whether inside this interval along the MS we observe as many stars as predicted. Let us assume that the LF does not change near the turnoff; we expect therefore to find as many stars in the 0.3 mag portion of the MS below the termination point as in the clump itself times the ratio of MS to clump

lifetime, which, from Flower's models, is ~ 3 . Between $M_V^{\text{MS}} = 0.8$ and $M_V^{\text{MS}} = 1.1$ one obtains 1100 stars from the LF of Table 2. This number is only half that observed in the clump and, therefore, a factor of 6 smaller than predicted. Since, on the other hand, the MS LF is likely to increase toward fainter magnitudes, and, in addition, the underlying younger MS should significantly contribute to the observed MS, we conclude that the clump population is drastically unaccounted for. There are far too many clump red giants, and a contribution from older stars must indeed be present. Notice that since we are dealing with stars in the MS and in the clump at essentially the same visual magnitude level, any unaccounted incompleteness in the data should affect both sequences equally, whereas any incompleteness as a function of blue magnitude should affect the redder clump population more—strengthening the foregoing argument even more.

We now turn to the determination of an upper age limit. Empirical information based on observations in the Galaxy can be used to set limits to the age (or mass) at which subgiants begin to populate the observational CMD. Inspection of the diagrams of clusters dated by Janes and Demarque (1983) shows that as age increases, the transition to a populated subgiant branch takes place somewhere between the ages of NGC 2420 and 2506 and that of M67, i.e., in the neighborhood of 3×10^9 yr. This age value is consistent with theoretical computations by Kinahan and Harm (1975), who have modeled the problem of the closure of the Hertzsprung gap as a function of mass and composition. A weak or nonexistent subgiant branch in our CMD would therefore indicate an upper age limit of $\sim 3 \times 10^9$ yr for the bulk of the observed population irrespectively of metallicity. We must ask then how strong is the observed subgiant branch, and how important is the contribution to it of MS and clump stars carried into the subgiant locus by the distribution of photometric errors over a sample as large as the one considered here. In order to model a representative section of the subgiant branch, let us take as reference a square region of dimension 0.2×0.2 mag centered at $V = 19.9$, $B - V = 0.8$. From Figure 6 such a square contains a total of 184 ± 14 stars (Poisson sampling error), which can represent either true subgiants or stars belonging to the MS and the clump. For a Gaussian distribution of stars centered at the clump with $\sigma_V = 0.3$ (Fig. 8) and containing 552 ± 23 stars inside a 0.2×0.2 mag square (Fig. 6), one predicts 77 ± 9 stars at a vertical distance $2\sigma_V = 0.6$ mag, i.e., inside the reference region. Furthermore, by assuming symmetry of the residuals, one expects as many stars on the red side of the mean locus of the MS along lines of constant B and V as on its blue side, i.e., a total of 72 ± 8 additional stars from Figures 5 and 6, giving a total contribution of 149 ± 16 stars to the observed population of the reference square. This number is a lower limit, however, since the MS is asymmetric in the direction of the subgiant branch because of the well-known extension toward the red of the core-hydrogen-burning MS phase. We conclude that within the errors the subgiant branch is essentially void or contains very few true members (fewer than 35 ± 21 inside the reference zone).

The main conclusion of this section is then that the bulk of star formation, as represented by the observed red giants, started earlier than about one billion years ago, and that

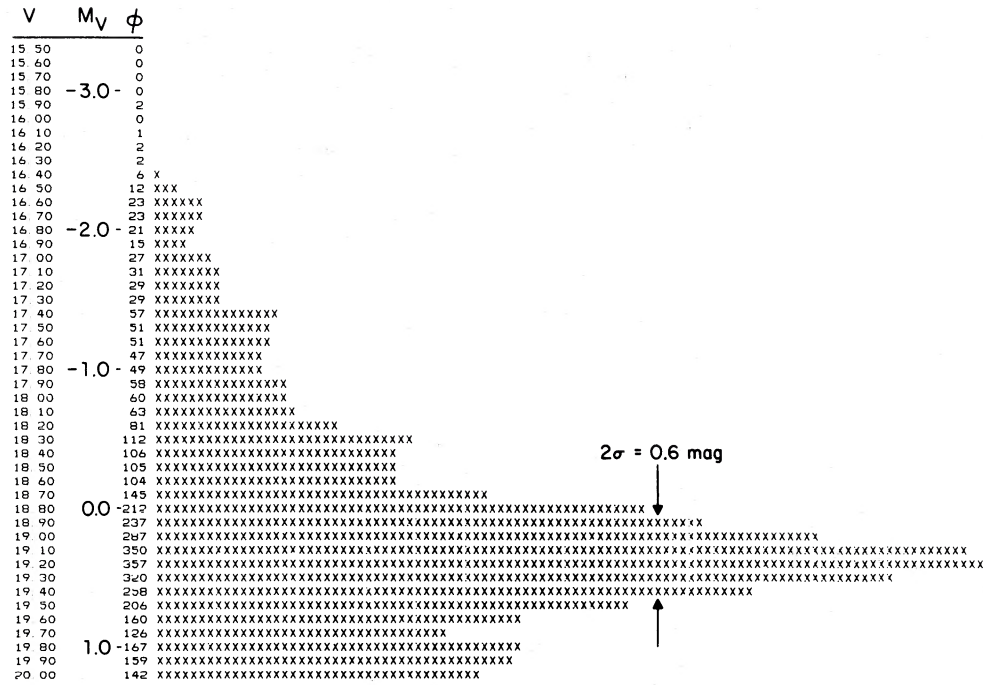


FIG. 8.—The red-giant differential luminosity function in histogram-like representation as a function of apparent and absolute magnitudes. The adopted width of the giant clump is indicated (see text).

stars are present which may have ages extending up to 3×10^9 yr, with very few objects, if any, older than this limit.

IV. SUMMARY AND CONCLUSIONS

Analysis of the morphology and stellar densities in the CMD combined with new evolutionary results pertaining to the core-helium-burning phase of evolution indicates that (1) stellar formation continues in the bar areas of the LMC; (2) an old Population II, such as that of the globular clusters of the Galaxy, is not a significant contributor to the observed CMD; and (3) the bulk of star formation, which continues to date, started earlier than about one billion years ago but not later than about three billion years ago. The precise rate of star formation as a function of time inside this age range is not known from our data. The possibility of bursts of star formation is not excluded. The conclusion that most of the observed giants are intermediate-age stars is strengthened by the presence of a populated upper AGB. However, uncertainties in the AGB models coupled to serious discrepancies with other dating procedures (Hodge 1983) prevent us from using the information on the extended giant branch in a more quantitative way. The observed population is, in any case, conspicuously different from that of the galactic disk in the neighborhood of the Sun (Wilson 1976; Hardy 1978a). It is also important to remark that the paucity of subgiants in the LMC field contrasts with the well-populated subgiant branch found in the SMC (Hardy and Durand 1984), which would then indicate an older age centroid for the SMC.

Our results are compatible with (but do not prove) the assertion (Stryker and Butcher 1981 and references therein) that a large-scale event triggered star formation in the LMC 2–4 billion years ago. We stress in this context the similarities between our (bright) MS luminosity function and those of Butcher (1977) and Stryker and Butcher (1981) far away from our region. Questions concerning the existence

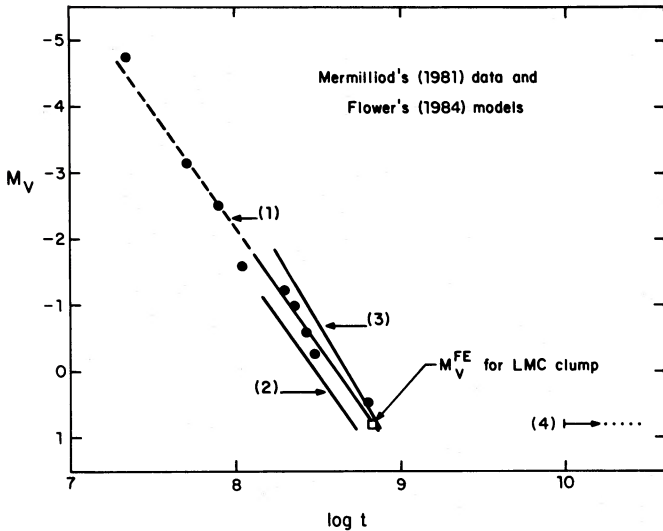


FIG. 9.—The core-helium-burning clump models from Flower (1984) (straight lines) are compared with the data from Mermilliod (1981b), shown as fitted circles, and with the position of the faint edge (FE) of the LMC clump. Mermilliod's data are for the mean position of the clump. Flower models are evaluated for the FE magnitudes and correspond to: (1) $[Fe/H] = -0.7$, (2) $[Fe/H] = -0.2$, and (3) $[Fe/H] = -1.0$; (4) indicates the mean position of the globular cluster horizontal branch. Model (1) has been extrapolated linearly into the region of the young clusters to show the observed consistency in slope (see text).

of a halo population projected against the bar cannot be answered with our data owing to the smallness of the area surveyed in this investigation. Neither can we exclude the presence of a *weak* Population II component since some RR Lyrae stars are known to exist in the LMC field (Graham 1973).

How representative of the bar as a whole are our results? The information in Table 1 and the colors of the central regions of the LMC (Fig. 1) reported by Hardy (1978*b*) indicate small variations in integrated properties over a surprisingly large section of the LMC of dimension 2×2 square degrees. Comparison of the bright end of our CMD with those of Hardy (1977, 1978*a*) confirms this result and suggests that most color differences can be attributed to the varying degree of contamination due to the patchy distribution of very young stars across the face of the area surveyed, superposed on a uniform underlying older disk population. Furthermore, our CMD can be compared with less populous brighter diagrams obtained by other workers as a by-product of cluster studies. Flower (1982) studied NGC 2058 and 2065, on the opposite side of the bar; his red-giant branch superposes well with ours when differences in reddening are taken into account, although his statistics for field stars over the magnitude range in common prevents a detailed comparison. In the case of Nelson and Hodge (1983), who studied NGC 1847, a young compact cluster next to our region, all we can conclude from the few field stars included in their CMD is that our respective photometric scales are consistent. To the extent that a bar acts as a population "smearer," this seeming uniformity in the underlying population of the central regions is not surprising. More surprising is the relatively young age of the bulk of the population, a characteristic shared by the cluster system (Flower 1984). If the generality of these results is further strengthened by other studies, it would seem that just a few billion years ago the LMC was basically a large gaseous mass.

We believe that we have essentially reached the resolution

limit of Earth-based photographic work in the LMC bar. CCD cameras may increase the magnitude limit over restricted areas by increasing the signal-to-noise ratio for contrast. But we do not foresee a dramatic improvement in the limiting magnitude for very crowded regions. Observations from the Space Telescope will, however, reach the turnoffs even in the most crowded regions of the bar, and one should wait until then to pursue this type of observations. A different, more astrophysical line of attack can be adopted at the present time. It is well known that direct measurements of stellar physical parameters can be accomplished through the use of narrow-bandpass photometric systems. For red giants use of the (41–42), (42–45), and (45–48) indices of the DDO system (see Hardy 1979 and references therein) can provide reliable values for the metallicity and the masses—and therefore ages—of clump stars. Use of properly calibrated panoramic detectors such as CCDs or large-format photon counters can provide images in narrow bandpasses comprising hundreds of stars for which the same profile-deconvolution photometric techniques used here can be applied. It is likely that such an approach applied to objects brighter than $V = 20$, which one of us (E. H.) intends to pursue, will settle the issues raised and partially answered in this investigation, in particular, that of the precise rate of star formation as a function of age.

E. H. and R. A. S. wish to thank the Carnegie Institution of Washington for observing time at Las Campanas. E. H. acknowledges a kind invitation from the Consiglio Nazionale delle Ricerche of Italy to spend part of the 1982 summer at the Rome Astronomical Observatory, where this and other projects were started, and the hospitality of Professor P. Giannone. E. H. also thanks P. J. Flower for communicating his results on evolutionary models for red giants in advance of publication. This investigation was partially financed by NSERC—Canada (E. H.); K. A. J. acknowledges support from NSF grant AST-8024069.

REFERENCES

- Aaronson, M., and Mould, J. 1982, *Ap. J. Suppl.*, **48**, 161.
 Arp, H., and Cuffey, J. 1962, *Ap. J.*, **136**, 51.
 Bijaoui, A. 1980, *Astr. Ap.*, **84**, 81.
 Buonanno, R., Buscema, G., Corsi, C. E., Ferraro, I., and Iannicola, G. 1983*a*, *Astr. Ap.*, submitted.
 Buonanno, R., Buscema, G., Corsi, C. E., Iannicola, G., and Fusi Pecci, F. 1983*b*, *Astr. Ap. Suppl.*, **51**, 83.
 Buonanno, R., Buscema, G., Corsi, C. E., Iannicola, G., Smriglio, F., and Fusi Pecci, F. 1983*c*, *Astr. Ap. Suppl.*, **53**, 1.
 Buonanno, R., Corsi, C. E., De Biase, G. A., and Ferraro, I. 1979, in *International Workshop on Image Processing in Astronomy*, ed. G. Sedmak, M. Capaccioli, and R. J. Allen (Osservatorio Astronomico di Trieste), p. 354.
 Buonanno, R., Corsi, C. E., and Fusi Pecci, F. 1981, *M.N.R.A.S.*, **150**, 11.
 Butcher, H. 1977, *Ap. J.*, **216**, 372.
 Cannon, R. D. 1970, *M.N.R.A.S.*, **150**, 111.
 Ciardullo, R. B., and Demarque, P. 1977, *Trans. Yale Obs.*, Vol. 33.
 Cowley, A. P., and Hartwick, F. D. A. 1982, *Ap. J.*, **259**, 89.
 Flower, P. J. 1982, *Pub. A.S.P.*, **94**, 894.
 ———. 1984, *Ap. J.*, **278**, 582.
 Graham, J. 1973, in *IAU Colloquium 21, Variable Stars in Globular Clusters and in Related Systems*, ed. J. D. Fernie (Dordrecht: Reidel).
 Hardy, E. 1977, *Ap. J.*, **211**, 718.
 ———. 1978*a*, *Ap. J.*, **223**, 98.
 Hardy, E. 1978*b*, *Pub. A.S.P.*, **90**, 132.
 ———. 1979, *A.J.*, **84**, 319.
 ———. 1981, *A.J.*, **86**, 217.
 Hardy, E., and Durand, D. 1984, *Ap. J.*, **279**, in press.
 Hardy, E., Melnick, J., and Rheault, C. 1980, in *IAU Symposium 85, Star Clusters*, ed. J. E. Hesser (Dordrecht: Reidel), p. 343.
 Hodge, P. 1982, *Ap. J.*, **256**, 447.
 ———. 1983, *Ap. J.*, **264**, 470.
 Janes, K., and Demarque, P. 1983, *Ap. J.*, **264**, 206.
 Kinahan, B. K., and Harm, R. 1975, *Ap. J.*, **200**, 330.
 Kormendy, J. 1981, in *The Structure and Evolution of Normal Galaxies*, ed. S. M. Fall and D. Lynden-Bell (Cambridge: Cambridge University Press), p. 85.
 Mermilliod, J.-C. 1981*a*, *Astr. Ap. Suppl.*, **44**, 467.
 ———. 1981*b*, *Astr. Ap.*, **97**, 235.
 Moffat, A. F. J. 1969, *Astr. Ap.*, **3**, 455.
 Sandage, A. 1957, *Ap. J.*, **125**, 422.
 ———. 1970, in *Pontificiae Accademiae Scientiarum Scripta Varia*, No. 35, p. 601.
 ———. 1982*a*, *Ap. J.*, **252**, 553.
 ———. 1982*b*, *Ap. J.*, **252**, 574.
 Sandage, A., and Tammann, G. A. 1971, *Ap. J.*, **176**, 293.
 Stryker, L. L. 1983, *Ap. J.*, **266**, 82.

Stryker, L. L., and Butcher, H. R. 1981, in *IAU Colloquium 68, Astrophysical Parameters for Globular Clusters*, ed. A. G. D. Philip and D. S. Hayes (Schenectady: L. Davis Press), p. 225.

Stryker, L. L., Butcher, H. R., and Jewell, J. L. 1981, in *IAU Colloquium 68, Astrophysical Parameters for Globular Clusters*, ed. A. G. D. Philip and D. S. Hayes (Schenectady: L. Davis Press), p. 267.

Tift, W. G., and Snell, C. M. 1971, *M.N.R.A.S.*, **151**, 365 (TS).

Tody, D. 1980, *Proc. Soc. Photo-Opt. Instrum. Eng.*, **264**, 171.

van den Bergh, S. 1974, *Ap. J.*, **193**, 63.

Wilson, O. C. 1976, *Ap. J.*, **205**, 823.

ROBERTO BUONANNO and CARLO E. CORSI: Osservatorio Astronomico di Roma, Sede di Monte Mario, Viale del Parco Mellini, 84. 00136, Roma, Italy

EDUARDO HARDY: Département de physique, Faculté des Sciences et génie, Université Laval, Cité Universitaire, G1K 7P4, Québec, Canada

KENNETH A. JANES: Astronomy Department, Boston University, 725 Commonwealth Ave., Boston MA 02215

ROBERT A. SCHOMMER: Department of Physics and Astronomy, Rutgers University, P.O. Box 849, Serin Physics Laboratory, Piscataway, NJ 08854